

Sexual Dimorphism of the First Rib: A Comparative Approach Using Metric and Geometric Morphometric Analyses*

Jeffrey James Lynch,¹ M.Sc.; Peter Cross,² M.Sc.; and Vivienne Heaton,³ PhD

¹Defense POW/MIA Accounting Agency, Offutt Air Force Base, Omaha, NE.

²School of Forensic and Investigative Sciences, University of Central Lancashire, Maudland Building,
Room 137, Preston PR1 2HR, U.K.

³School of Physical and Geographical Sciences, Keele University, Keele, Staffordshire, U.K.

*This paper does not reflect the opinion of the Defense POW/MIA Accounting Agency.

ABSTRACT: This research investigated the sexual dimorphism of the first human rib using geometric morphometric and metric approaches on a sample of 285 specimens containing European Americans and African Americans from the Hamann-Todd collection. Metric measurements were investigated for sexual dimorphism and ancestral differences using univariate statistics. Four type II landmarks and 40 sliding semi-landmarks were placed outlining the dorsal and ventral curvatures of the ribs. Landmark data were processed using Generalized Procrustes analyses with Procrustes distance sliding, and the subsequent coordinates were investigated for sexual dimorphism and ancestral differences using Procrustes ANOVAs. Both geometric morphometric and metric data were analyzed using cross-validated discriminant function analyses to test the hypothesis that variables from both approaches can be combined to increase sex classification rate. European Americans had sex correctly classified as high as 88.05% and African Americans as high as 70.86% using a combination of metric and geometric morphometric variables.

KEYWORDS: forensic science, forensic anthropology, geometric morphometrics, first rib, shape analysis, sexual dimorphism, ancestry, discriminant function analysis, sliding semi-landmarks, landmark error

Research on sex estimation from complete ribs is lacking in the field of forensic anthropology. The majority of rib studies have focused on the sternal end using degenerative and metric analyses to estimate age and sex respectively (1-4). Very few studies have focused on the morphology of ribs in their entirety, and even less provided adequate samples to evaluate the practicality of sex estimation among and between ancestral populations (5,6).

Over the last decade geometric morphometric analysis has become popular among physical anthropologists as a method to analyze biological information using the shape and size of skeletal elements (7-9). However, these studies ignored the potential resource of metric analysis and focused on a pooled ancestral category. Both metric and geometric morphometric studies within forensic anthropology have utilized a single methodological framework to evaluate biological information. Within physical anthropology, the majority of geometric morphometric research has focused on the pelvic and cranial regions given their history as being sexually dimorphic (10). While this has yielded significant results (7,8), research on other post-cranial elements has been overlooked.

Given that bones develop and remodel under the influence of several factors (11), using a single method ignores potential biological information that can increase classification accuracy. At a time when forensic anthropology is gaining popularity and is under scrutiny (12), higher classification rates are critical. This study highlights the importance of combining methodologies, focusing on previously overlooked skeletal elements, and accounting for ancestral differences when attempting to develop new practical methods in forensic anthropology.

Materials and Methods

The sample used in this study is from the Hamann-Todd Osteology Collection. Selection criteria included left first ribs free of ossified cartilage that obstructed the ventral and dorsal margins of the sternal end. Any specimens exhibiting congenital abnormalities were not used. Ribs were selected on the basis of exhibiting fully developed adult anatomy. The developmental stage was determined by the fusion of the rib head epiphyseal flake, which fuses between 17 to 25 years of age (11,13). In total 285 individuals were selected for use, consisting of 134 European Americans (EA) between 18 to 87 years of age and 151 African Americans (AA) between 18 to 89 years of age. A balance between sexes was maintained within each population (Table 1).

Four measurements from each rib were taken in millimeters (Figure 1). The first measurement was the total length (TL), taken by placing the rib head and tubercle against the vertical fixed wall of an osteometric board and measuring to the ventral most point with the superior surface of the rib facing upward. If the rib head and tubercle did not rest flat against the vertical wall, the rib was positioned so the tubercle and neck made contact. The second measurement was the maximum ventral-dorsal diameter (VD), taken at the scalene tubercle using Fowler high precision vernier calipers. The third measurement was the dorsal curvature (DC), taken from sternal end to the start of the rib head. The fourth measurement was the tuberculoventral arc (VA), taken from the sternal end to the start of the tubercle (14). A flexible tape measure warped to the contour of curvature was used to take the latter two measurements.

Photographs of each rib were taken using an Olympus E-PL5 camera at 4608 x 3456 resolution. The camera was mounted on a photography copy stand at a 90° angle looking downward on the superior surface of the rib. The top right frame of the camera was aligned at approximately 10 cm x 13.5 cm on a

Wizthings Photographic Scale III. This guaranteed that any camera distortion occurred at the same location within each photograph to reduce the introduction of variation from distortion. To reduce barrel distortion, the camera kit lens was set at 42 mm and the camera placed approximately 48 cm above the photograph scale. Each specimen was placed at approximately 10 cm x 2 cm with the head and tubercle placed against the 10 cm line and the ventral curvature placed against the 2 cm line. An L-shaped foam block was placed along the scale lines to position every specimen in the same orientation.

Both type II and semi-landmarks were chosen for this project (Figure 1). Type II landmarks are defined by relative geometry, such as a maximum point along a curvature (15,16). The type II landmarks included the ventral and dorsal margins at the sternal end, visually the end of the ventral curvature at the rib tubercle, and the most superior point on the rib head in the orientation of the photograph. These landmarks served as anchoring points for the semi-landmarks. In total 40 semi-landmarks were used with 20 placed on each curvature.

Each photograph was processed using the Makefan8 software which superimposes fan shaped lines to aid in landmark placement (17). Two fans were created for each specimen to account for semi-landmarks on both curvatures (Figure 2). The type II landmarks were used at the ends of the fans to guarantee the semi-landmarks were placed approximately equally spaced between their anchoring points.

After each specimen had fans superimposed, the images were digitized using the Geomorph package for R (18). The process of digitization included adding a digital scale on each photograph. To avoid introducing scale error from camera distortion, all scales were set between 0.5 cm and 1 cm at the 7.5

cm intersection. The scale factors were set at five, indicating that between the scale end points there were five data points translating to 1 mm increments on the photograph scale.

European American and African American digitized coordinates were subjected to separate and combined Generalized Procrustes Analyses (GPA), in the Geomorph package for R, producing three sets of Procrustes coordinates. These three sets of Procrustes coordinates allowed the comparison of ancestral samples and the separate testing of each ancestral sample. The GPAs incorporated Procrustes distance sliding for the semi-landmarks to create homologous landmarks across all data sets. Centroid sizes were extracted from Cartesian data for both ancestries and were appended to matrices of Procrustes coordinates to create form variables that account for both shape and size.

Potential shape outliers were identified by plotting all specimens sequentially from their Procrustes distance to the mean. Any specimen above or below the interquartile range was labeled as a potential outlier. Similarly, potential centroid size and measurement outliers were identified using boxplots labeling data that were 1.5 times the interquartile range. This was done within the European American and African American samples separately. The identified specimens were removed and all analyses were performed again to test the influence of each potential outlier. In this study no potential outliers were removed from the final analyses due to a lack of influence.

This study took a different approach to analyzing landmark error. Measuring landmark error in geometric morphometrics is problematic due to each landmark having x and y coordinate values. Further, after registering landmarks to a coordinate system, such as Procrustes coordinates from a GPA, landmark error is reduced (19). During the rotation, translation, and scaling of each specimens landmark configuration, error at each landmark is spread out across the entire configuration as it is treated like

shape variation reducing the actual error. The error from Procrustes coordinates is relative to that configuration and cannot be compared to other studies. Due to these issues, this project took a different approach by looking at the x and y values from Cartesian coordinates separately to avoid reducing error from the GPA and allowing the comparison of error between x and y values within a single landmark. Scaling the Cartesian coordinates to a common metric unit and analyzing them with the technical error of measurement (TEM) allowed a better representation of inter- and intra-observer error. The scaled error will allow the landmark precision in this project to be compared with future geometric morphometric studies in a common metric unit rather than project specific coordinates.

Inter- and intra-observer error analyses for measurement repeatability were assessed by having three graduate students, trained in osteology and forensic anthropology, take measurements from four specimens on three different occasions separated by a day. Inter- and intra-observer landmark error were assessed by having the author and one participant digitize the four type II landmarks on four specimens randomly selected from the study on four different occasions. The participation of graduate students was approved by the University of Central Lancashire's Ethics Committee. Given that the semi-landmarks were dependent on the four type II landmarks, only type II were digitized for error analysis. The Cartesian coordinates were scaled to represent millimeters and the x and y values from the type II landmarks were used for analysis. The landmark and measurement data were analyzed to assess the TEM for multiple observers or more than two replicates from a single observer. Below is the version of the TEM formula where K can be the number of observers or replicates, N the sample size, M the measurement, and $M(n)$ is the n th replicate of measurement (20):

$$\sqrt{\frac{\sum_1^N \left[\left(\sum_1^K M(n)^2 \right) - \frac{\left(\sum_1^K M(n) \right)^2}{K} \right]}{N(K-1)}}$$

To account for ancestral differences, each measurement was tested independently using a one-way analysis of variance (ANOVA) to test for statistical differences among the same sex between European American and African American samples. This was done to avoid introducing sexually dimorphic variation into the analyses. Due to significant results from those tests, each measurement was tested independently using a one-way ANOVA to test for statistical differences between sexes within each ancestral sample. The statistical assumptions of normality and equal variance were tested using quantile-quantile plots of residuals and Levene's tests respectively. Measurements not meeting the normality assumption were transformed with a power function by trial and error and retested until normality assumptions were met. If there were significant differences between sexes, the measurements were used in discriminant function analyses using leave-one-out cross-validation to test for sex classification rate within each ancestral sample. The statistical assumptions of normality and homogeneity of variance were previously met in the sexual dimorphism analyses given that only one predictor variable was used per discriminant function analysis and any previous transformations were used.

To account for ancestral differences, Procrustes coordinates from the combined GPA were subjected to Procrustes ANOVAs to test for statistical differences among the same sex between European American and African American samples. Similarly, centroid sizes from the combined sample were tested using one-way ANOVAs to test for statistical differences among the same sex between ancestries. Based on the results of the ancestral analyses, the subsequent statistical analyses for sexual dimorphism were conducted on each ancestral sample separately. The Procrustes coordinates from European American and African American samples were subjected to Procrustes ANOVAs to test for statistically significant differences between sexes. Similarly, the centroid sizes were subjected to one-way ANOVAs to test for

statistically significant differences between sexes. The assumptions of normality and equal variance for centroid sizes were tested using quantile-quantile plots of residuals and Levene's tests respectively. Centroid sizes not meeting the normality assumption were transformed with a power function by trial and error and retested until normality assumptions were met. Testing for statistical significance between ancestral groups and sexes using form was not carried out as the previous analyses on shape and centroid size established the differences.

Dimensionality reduction was carried out using principal component analyses on each set of Procrustes coordinates and form in order to reduce the number of variables to avoid violating the assumptions of a discriminant analysis. Any principal component score not having near-zero variance was used to account for as much discriminable variation as possible. Near-zero variance means that the variance across the predictor variable is near-zero and does not represent enough variation to be useful in discriminating between groups. Near-zero variance was determined in the LDA function in the MASS package for R (21).

The principal component scores from Procrustes coordinates and form data, and centroid sizes, were subjected to separate discriminant function analyses using leave-one-out cross-validation to test for classification rates between sexes for European American and African American samples. Box's M-test and Royston's test with Chi-squared quantile-quantile plots, from the biotools (22) and MVN (23) R packages respectively, were used to assess homogeneity of covariance and multivariate normality to meet the assumptions of a discriminant analysis with multiple predictor variables. Box's M-test was used with a significance level of 0.001, as opposed to the standard p-value of 0.05, given that it is highly sensitive and it has been recommended any value greater than 0.001 be ignored (24).

Data from the metric and geometric morphometric approaches were combined in discriminant function analyses to assess classification accuracy. Each measurement was combined with shape, form, and centroid size. Box's M-test and Royston's test with Chi-squared quantile-quantile plots were used to assess homogeneity of covariance and multivariate normality. Any combination failing the normality test had the measurement data transformed with a power function by trial and error and retested until normality assumptions were met. All statistical analyses were carried out in the R software version 3.2.0 for Linux (25).

Results

Inter- and intra-observer error showed minimal TEM across all measurements and type II landmarks (Tables 2,3). Therefore, the results of this study were unlikely to have been influenced by observer error. The mean and standard deviation of the measurements and centroid sizes are given in Table 4. The mean shapes for each sex, ancestry, and total variation from all three GPAs are illustrated in Figures 3, 4, and 5.

There were statistically significant differences between European American females and African American females in the VD and VA measurements. Similarly, there were statistically significant differences between European American males and African American males in the VD measurement. Among shape variables, there were statistically significant differences between European American males and African American males, and European American females and African American females. Centroid size variables showed no statistically significant difference between European American males and African American males. Similarly, there were no statistically significant centroid size differences between European American females and African American females. Table 5 lists the statistical significance of each analysis. Due to these differences each ancestry was analyzed separately for sexual

dimorphism. Thin-plate spline deformation grids were utilized to show the mean shape from the combined GPA deformed to the mean of each sex from each ancestry (Figure 6).

There were statistically significant differences between European American males and females in the TL, VD, DC, and VA measurements. Similarly, there were statistically significant differences between African American TL and VD measurements. Among shape and centroid size variables, there were statistically significant differences between European American males and females, and African American males and females. Table 6 lists the statistical significance of each analysis. Based on these results, shape variables, centroid size, TL, and VD measurements were utilized in discriminant analyses for both ancestries and additionally the DC and VA measurements for European Americans. Thin-plate spline deformation grids were utilized to show the mean shape from each ancestral GPA deformed to the mean of each sex (Figure 7).

Results from the separate principal component analyses included the first four principal components from each analysis. For the European American coordinates, the first four principal components accounted for 78.23% of the total variation with principal component 1 (PC1) accounting for 41.48%, principal component 2 (PC2) accounting for 17.77%, principal component 3 (PC3) accounting for 13.54%, and principal component 4 (PC4) accounting for 5.4% of the variation. For the African American coordinates, the first four principal components accounted for 80.17% of the total variation with PC1 accounting for 47.99%, PC2 accounting for 16.89%, PC3 accounting for 10.17%, and PC4 accounting for 5.1% of the variation.

Form data, created from appending the centroid sizes as additional columns to the European American and African American Procrustes coordinates, were subjected to separate principal component analyses. The principal component scores included the first four principal components from each analysis. For the European American form data, the first four principal components accounted for 90.64% of the total variation with PC1 accounting for 66.46%, PC2 accounting for 13.44%, PC3 accounting for 5.98%, and PC4 accounting for 4.76% of the variation. For the African American form data, the first four principal components accounted for 91% of the total variation with PC1 accounting for 66.4%, PC2 accounting for 15.04%, PC3 accounting for 6.11%, and PC4 accounting for 3.45% of the variation.

In total 30 discriminant function analyses were performed using a combination of shape, form, centroid size, and metric variables that showed statistically significant sexual dimorphism in the previous ANOVAs. The sex classification rates ranged from 58.27% to 88.05%. Among European Americans shape combined with VA had the highest classification rate of 88.05%. Among African Americans shape combined with TL had the highest classification rate of 70.86%. Table 7 lists the cross-validated classification rates for each analysis.

Discussion

Ancestral differences in shape occur along the dorsal and ventral curvatures with African Americans having a wider rib in the ventral-dorsal direction and wider ventral curvature with greater angle. However, European Americans had a wider dorsal curvature with greater angle than African Americans. The deformation grids showed females from both ancestries had a greater degree of deformation indicating the difference between ancestries primarily occurred among females. In males the difference was subtle with only slight deformation. The greater shape differences among African Americans explain

the statistically larger VA measurement among African American females and the larger VD measurement among African American males and females when compared to European Americans.

Centroid size data showed no statistical difference between ancestries. However, the female centroid size significance value was 0.05, indicating uncertainty. More data may yield different results. Based on the current data, the primary difference between European Americans and African Americans occurred in shape, not size. The absence of centroid size influence indicated that the statistically significant differences in the VD and VA measurements are due to the difference in shape and not size. The TL measurement accounted for multiple locations on the extremities of the rib including the head, tubercle, neck, and sternal end making it more likely to detect a difference in size. The lack of statistical difference among the TL measurement corroborates the centroid size results showing no statistical difference.

Between sexes within each ancestry, shape variation showed sexually dimorphic differences along the dorsal and ventral curvatures. Males displayed a wider rib in the ventral-dorsal direction, sharper dorsal curvature with a lesser angle, and a wider ventral curvature with a greater angle compared to females. This type of sexually dimorphic variation was the same across ancestries, but the significance of the variation differed, with European Americans showing more sexually dimorphic variation. This was evidenced in the deformation grids, which showed greater deformation among European Americans with only slight deformation among African Americans. This corresponds to the Procrustes coordinate plots showing more mean shape deviation among European Americans, with less shape deviation among African Americans. This indicated the difference between ancestries appeared to be in the amount of sexual dimorphism exhibited.

The sexually dimorphic shape differences explained the statistical differences in the VD, DC, and VA measurements for European Americans and the VD measurement for African Americans. European American males had a wider rib, sharper dorsal curvature, and wider ventral curvature increasing the VD, DC, and VA measurements compared to females. Similarly, African American males had a wider rib, sharper dorsal curvature, and wider ventral curvature, but due to the less sexually dimorphic differences, only the VD measurements showed statistical differences. Centroid size data showed statistically significant differences between sexes among both ancestries. These results indicated that the overall size of the first rib, and not just the shape, contributed to the sexual dimorphism and statistically different metric measurements. Given that the TL measurement accounted for multiple extremities of the first rib, the centroid size results explained the statistical difference in TL measurements and both corroborated that sexual dimorphism exists in size for both ancestries.

Results from the discriminant function analyses further iterate the sexually dimorphic differences among and between ancestries. European Americans had the best sex classification performance with a high of 88.05% and African Americans had relatively poor performance with a high of 70.86%. Among European Americans, shape had high performance, form had moderate performance, and centroid size had poor performance indicating shape was the most sexually dimorphic variable. Among African Americans the performance of shape, centroid size, and form were relatively similar with form having a slightly higher performance. Furthermore, these performances were poor compared to European Americans, indicating African Americans were significantly less sexually dimorphic in shape and size.

Comparing both approaches, geometric morphometrics accounted for more variation and had better discrimination performance for European Americans. However, for African Americans, geometric morphometrics only had a better performance for form data with shape and centroid size being

comparable to the metric measurements. Statistically combining variables from both approaches produced performance increases. The highest overall increase in performance was 11.92% among African Americans, reflecting how two variables with poor performance, 64.9% and 58.94%, can be combined to increase the classification rate. The highest increase in performance for European Americans was 7.46%, producing the best discrimination performance overall. Overlap of quantifiable sexually dimorphic variation was likely introduced into the analyses, resulting in smaller discriminant performance increases. The corresponding relationship between mean shape differences and the metric measurements indicated that both variable types accounted for the same variation resulting in smaller performance increases. Further, there were three combinations producing a decrease in performance. Among European Americans the decrease in performance occurred with centroid size combined with the TL measurement. Among African Americans the decrease in performance occurred with centroid size and form, each combined with the VD measurement. This reflects the less sexually dimorphic variation in size for European Americans and overall less sexual dimorphism for African Americans. These combinations introduced random variation into the analyses making the actual sexually dimorphic variation less likely to be discriminated.

Individually, geometric morphometrics had better performance compared to the metric approach. Combining variables from both approaches provided statistical evidence that both methods can be used together to increase classification rates. Further, geometric morphometrics provided a way to visualize the metric differences, allowing a better understanding of the statistical measurement differences. Both methods complemented each other by providing different ways to analyze and understand the same sexually dimorphic variation. Geometric morphometrics provides an incredibly powerful tool to detect biological differences and the full impact of this method in forensic anthropology has yet to be seen. However, geometric morphometrics proved to be a time-consuming method making it, to date,

impractical in forensic science application. The placement of all landmarks in this project took approximately two weeks of work. Research into the development of user-friendly geometric morphometric software packages is required before this type of research becomes a method in practice. However, the results of this project support that geometric morphometrics combined with a metric approach can be used to achieve sex classification rates high enough to justify further research.

Acknowledgements

We would like to express our gratitude to Lyman Jellema from the Cleveland Museum of Natural History for access to the Hamann-Todd collection and the graduate students who participated in the error analysis.

References

1. Kunos CA, Simpson SW, Russell KF, Herschkovitz I. First rib metamorphosis: its possible utility for human age-at-death estimation. *Am J Phys Anthropol* 1999;110:303–23.
2. Kurki H. Use of the first rib for adult age estimation: a test of one method. *International Journal of Osteoarchaeology* 2005;15:342–50.
3. DiGangi EA, Bethard JD, Kimmerle EH, Konigsberg LW. A new method for estimating age-at-death from the first rib. *Am J Phys Anthropol* 2009;138:164–76.
4. Macaluso JP, Rico A, Santos M, Lucena J. Osteometric sex discrimination from the stern extremity of the fourth rib in a recent forensic sample from Southwestern Spain. *Forensic Sci Int* 2012;223:375.e1–375.e5.
5. Lanier RR. Length of first, twelfth, and accessory ribs in America whites and negroes; their relationship to certain vertebral variations. *Am J Phys Anthropol* 1944;2(2):137–46.
6. Elrod P. The potential of the angle of the first rib, head to tubercle, in sexing adult individuals in forensic contexts [Master's thesis]. Baton Rouge, LA: Louisiana State University, 2012.
7. Pretorius E, Steyn M, Scholtz Y. Investigation into the usability of geometric morphometric analysis in assessment of sexual dimorphism. *Am J Phys Anthropol* 2006;129:64–70.
8. Anastasiou E, Chamberlain AT. The sexual dimorphism of the sacro-iliac joint: an investigation using geometric morphometric techniques. *J Forensic Sci* 2013;58(S1):S126–34.
9. Efthymia N. Quantitative assessment of the sternal rib end morphology and implications for its application in aging human remains. *J Forensic Sci* 2013;58(2):324–9.
10. Spradley KM, Jantz RL. Sex estimation in forensic anthropology: skull versus postcranial elements. *J Forensic Sci* 2011;56(2):289–98.

11. Scheuer L, Black S. Developmental juvenile osteology. Oxford, U.K.: Academic Press, 2000.
12. Christensen AM, Crowder CM. Evidentiary standards for forensic anthropology. *J Forensic Sci* 2009;54(6):1211–6.
13. McKern TW, Stewart TD. Skeletal age changes in young American males, analyzed from the standpoint of age identification. Natick, MA: Headquarters Quartermaster Research and Development Command, 1957 Technical Report EP-45.
14. Gomez-Olivencia A, Eaves-Johnson KL, Franciscus RG, Carretero JM, Arsuaga JL. Kebara 2: new insights regarding the most complete Neandertal thorax. *J Hum Evol* 2009;57:75–90.
15. Bookstein FL. Morphometric tools for landmark data: geometry and biology. Cambridge, U.K.: Cambridge University Press, 1991.
16. Bookstein FL. Landmark methods for forms without landmarks: morphometrics of group differences in outline shape. *Med Image Anal* 1996;1:225–43.
17. Sheets DH. MakeFan8: tool for drawing “fans” or guidelines for digitizing semi-landmarks on images, 2014; <http://www3.canisius.edu/~sheets/morphsoft.html>.
18. Adams DC, Castillo EO. Geomorph: an R package for the collection and analysis of geometric morphometric shape data. *Methods in Ecology and Evolution* 2013;4:393–9.
19. Cramon-Taubadel NV, Frazier BC, Lahr MM. The problem of assessing landmark error in geometric morphometrics: theory, methods, and modifications. *Am J Phys Anthropol* 2007;134:24–35.
20. Goto R, Mascie-Taylor CGN. Precision of measurement as a component of human variation. *J Physiol Anthropol* 2007;26(2):253–6.
21. Venables WN, Ripley BD. Modern applied statistics with S. 4th ed. New York, NY: Springer, 2002.
22. Silva AR. Biotools: tools for biometry and applied statistics in agricultural science, 2015. <https://cran.r-project.org/web/packages/biotools/index.html>.

23. Korkmaz S, Goksuluk D, Zararsiz G. MVN: an R package for assessing multivariate normality. *The R Journal* 2014;6(2):151–62.
24. Tabachnick BG, Fidell LS. *Using multivariate statistics*. Boston, MA: Allyn and Bacon, 2001.
25. R Core Team. *R: a language and environment for statistical computing*. Vienna, Austria: R Foundation for Statistical Computing, 2015.

Additional information and reprint requests:

Jeffrey James Lynch, M.Sc.

Defense POW/MIA Accounting Agency

Offutt Air Force Base

Omaha, NE 68113

E-mail: jjlynch@bioarch.net

TABLE 1—*The distribution of age, sex, and ancestry of the sample.*

	Mean age	STD	Sample size
<i>EA Females</i>	44	15.52	64
<i>EA Males</i>	37	10.42	70
<i>EA Combined</i>	40	13.50	134
<i>AA Females</i>	36	14.53	72
<i>AA Males</i>	33	9.34	79
<i>AA Combined</i>	34	12.15	151

TABLE 2—*TEM* in mm for the TL, VD, DC, and VA measurements among participants for intra-observer error and combined for inter-observer error.

	TL	VD	DC	VA
Participant 1	1.32	0.50	1.96	2.97
Participant 2	0.65	0.65	1.78	2.86
Participant 3	1.87	0.57	1.63	1.55
Combined	1.30	0.60	2.07	2.44

TABLE 3—*TEM in mm for x and y Cartesian coordinate values from landmarks 1, 22, 23, and 44 among participants for intra-observer error and combined for inter-observer error.*

	Landmark 1		Landmark 2		Landmark 23		Landmark 44	
	X	Y	X	Y	X	Y	X	Y
Participant 1	0.09	0.11	0.14	0.06	0.07	0.07	0.09	0.18
Participant 2	0.23	0.15	0.16	0.19	0.21	0.24	0.17	0.25
Combined	0.17	0.44	0.18	0.46	0.37	0.42	0.34	0.26

TABLE 4—Mean and standard deviation for TL, VD, DC, and VA measurements, and centroid size.

	Males		Females	
	Mean	STD	Mean	STD
EA TL	80.26	5.88	74.46	7.77
EA VD	19.88	2.44	18.29	2.16
EA DC	89.31	7.28	86.83	8.32
EA VA	104.91	9.42	100.4	10.30
AA TL	80.35	5.94	75.93	5.98
AA VD	21.30	2.66	20.40	2.47
AA DC	88.89	7.32	86.44	8.75
AA VA	106.91	10.00	104.90	11.93
EA centroid size	183.49	13.31	170.91	14.20
AA centroid size	183.97	14.25	175.97	15.49

TABLE 5—Results of one-way ANOVAs for the TL, VD, DC, and VA measurements, shape and centroid size variables between ancestries. Bold indicates statistically significant differences.

	Ancestral differences		
	df	F statistic	p-value
Male TL	1	0.01	0.92
Male VD	1	10.63	< 0.05
Male DC	1	0.16	0.69
Male VA	1	1.56	0.21
Female TL	1	1.55	0.21
Female VD	1	26.43	< 0.001
Female DC	1	0.15	0.70
Female VA	1	5.47	< 0.05
Female centroid size	1	3.80	0.05
Male centroid size	1	0.02	0.88
Male shape	1	4.12	< 0.05
Female shape	1	11.16	< 0.05

TABLE 6—Results of one-way ANOVAs for the TL, VD, DC, and VA measurements, shape and centroid size variables between sexes. Bold indicates statistically significant differences.

	Sexual dimorphism		
	df	F statistic	p-value
EA TL	1	23.57	< 0.001
EA VD	1	14.10	< 0.001
EA DC	1	4.50	< 0.05
EA VA	1	7.91	< 0.05
AA TL	1	20.69	< 0.001
AA VD	1	4.56	< 0.05
AA DC	1	3.48	0.06
AA VA	1	1.26	0.26
EA centroid size	1	28.05	< 0.001
AA centroid size	1	11.78	< 0.001
EA shape	1	6.08	< 0.001
AA shape	1	2.62	< 0.05

TABLE 7—Summary of all sex discriminant analyses showing comparison within and between European American and African American samples. Bold text indicates 80% or higher. Change in performance for the combinations is provided in parentheses with + and - indicating increase and decrease respectively. NA indicates not applicable as those metric variables showed no statistical difference between sexes.

	European Americans	African Americans
TL	63.9%	64.9%
VD	62%	58.3%
DC	63.4%	NA
VA	59.7%	NA
Shape	80.59%	58.94%
Form	78.35%	70.19%
Centroid size	70.89%	59.60%
TL and shape	85.71% (+5.12%)	70.86% (+11.92%)
VD and shape	86.78% (+6.19%)	63.6% (+4.66%)
DC and shape	84.32% (+3.73%)	NA
VA and shape	88.05% (+7.46%)	NA
TL and form	81.20% (+2.85%)	66.89% (-3.3%)
VD and form	79.33% (+0.98%)	69.53% (-0.66%)
DC and form	79.85% (+1.5%)	NA
VA and form	79.85% (+1.5%)	NA
TL and centroid size	69.17% (-1.72%)	62.25% (+2.65%)
VD and centroid size	72.72% (+1.83%)	58.27% (-1.33%)
DC and centroid size	73.13% (+2.24%)	NA
VA and centroid size	71.64% (+0.75%)	NA

Figure and Legends

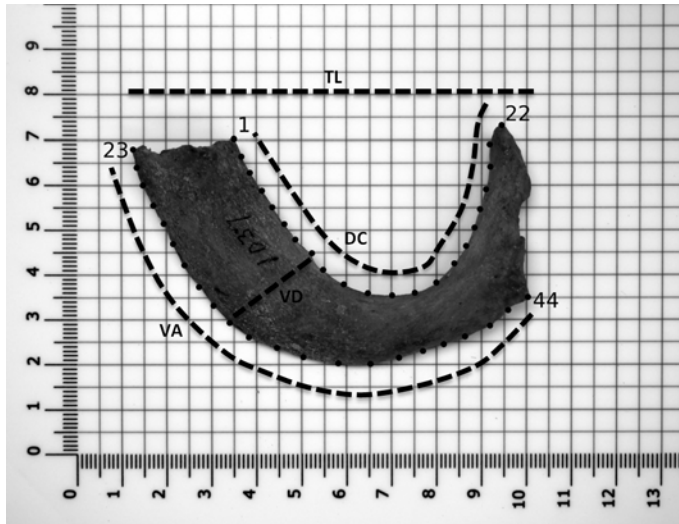


FIG. 1—Depicts the type II and semi-landmarks in sequential order from 1 to 44. The type II landmarks are numbered. The TL, VD, DC, and VA measurements are indicated by dashed lines. This photograph also illustrates the positioning of the ribs on the photographic scale.

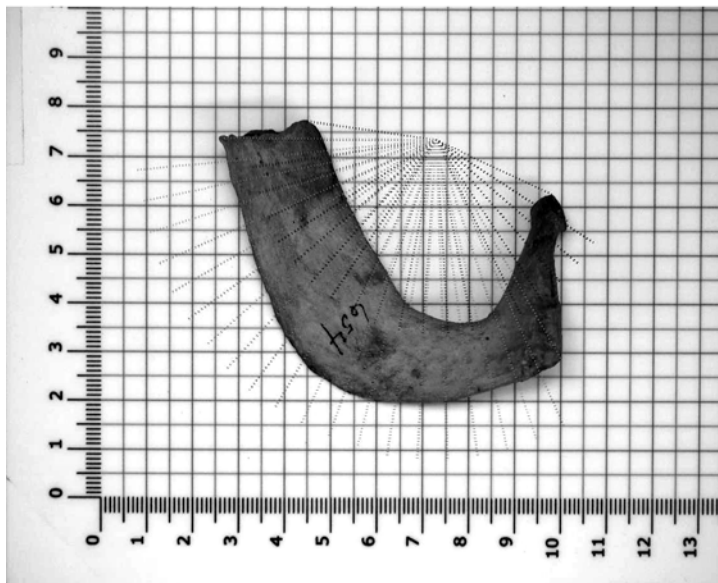


FIG. 2—Depicts fan superimposition over the specimen to aid in semi-landmark placement.

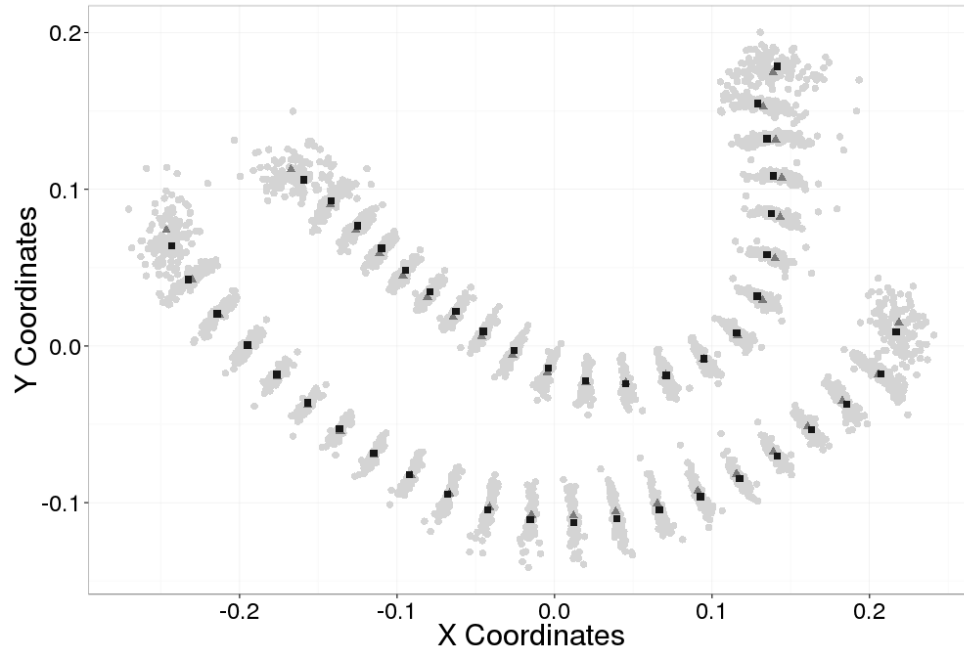


FIG. 3—Plot of European American Procrustes coordinates. Triangles indicate female mean shape, squares indicate male mean shape, and circles indicate total variation.

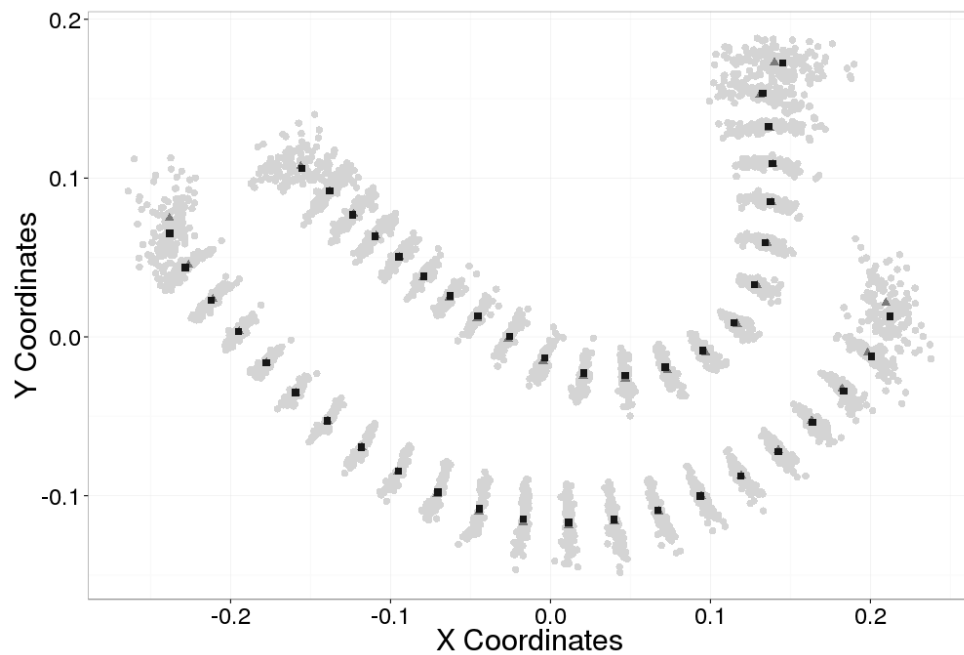


FIG. 4—Plot of African American Procrustes coordinates. Triangles indicate female mean shape, squares indicate male mean shape, and circles indicate total variation.

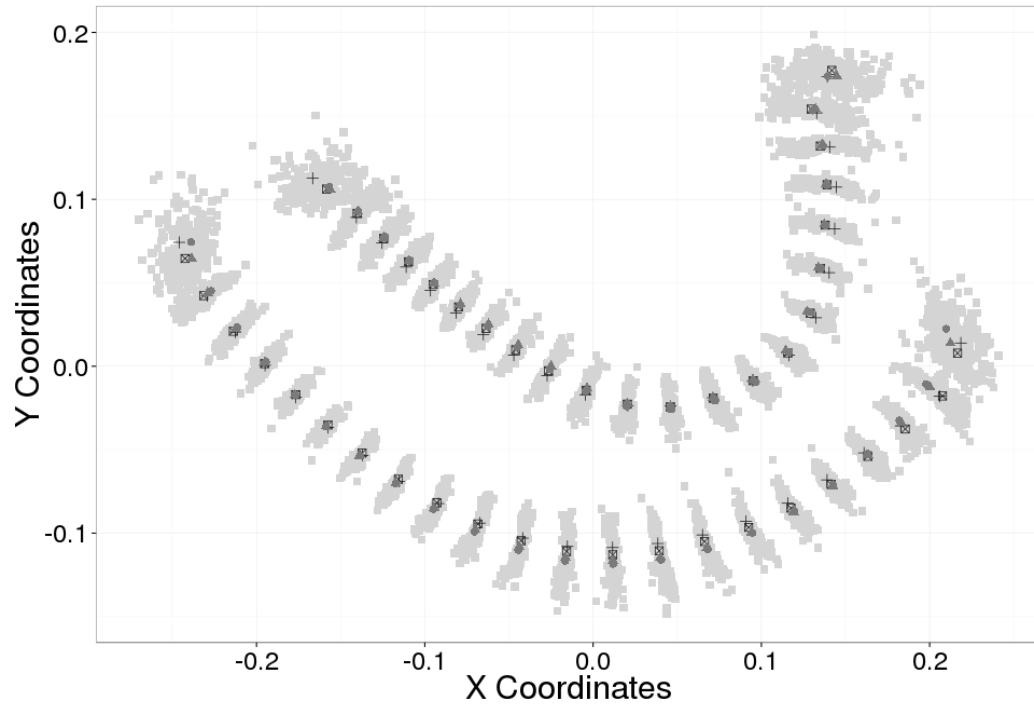


FIG. 5—Plot of Procrustes coordinates from the combined GPA. Circles indicate African American female mean shape, triangles indicate African American male mean shape, boxes with an x indicate European American male mean shape, crosses indicate European American female mean shape, and the filled squares indicate total variation.

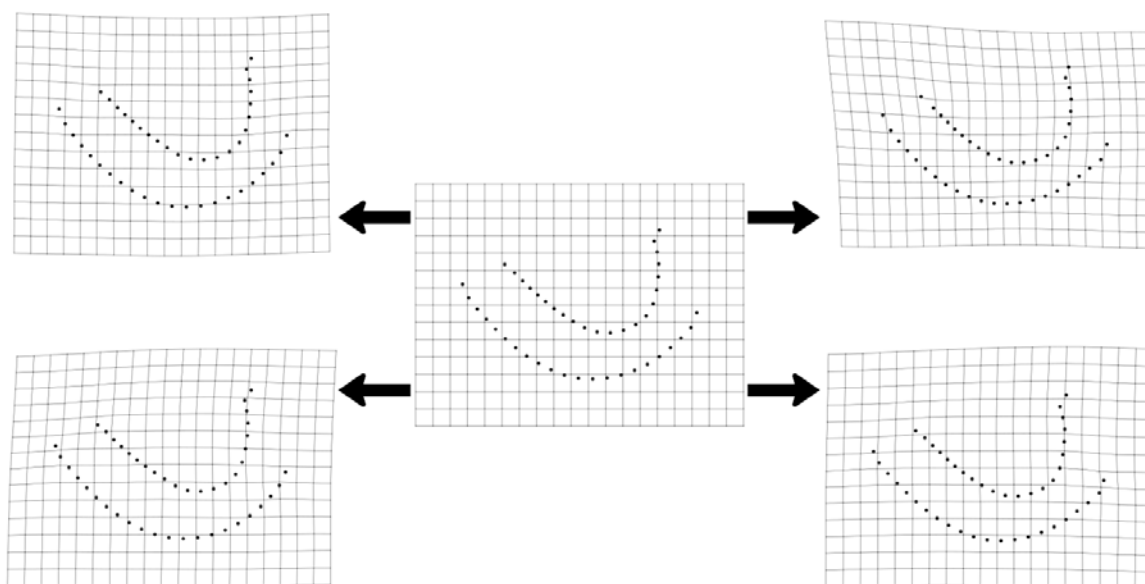


FIG. 6—Thin-plate spline deformation grids showing the mean shape (center) deformed to the mean European American female shape (top right), African American female shape (top left), European American male shape (bottom right), and African American male shape (bottom left).

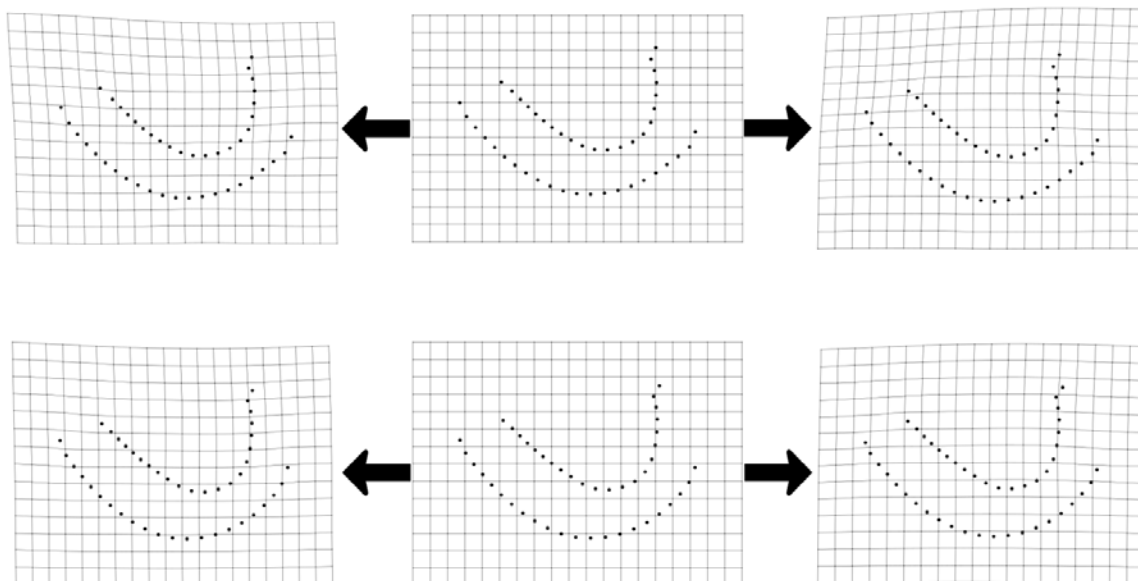


FIG. 7—Thin-plate spline deformation grids showing the European American mean shape (top center) deformed to the female mean shape (top left) and male mean shape (top right), and African American mean shape (bottom center) deformed to the female mean shape (bottom left) and male mean shape (bottom right).